

Developmental Cell, Volume 58

Supplemental information

Single nucleotide variants within heart enhancers dramatically increase binding affinity and disrupt heart development

Granton A. Jindal, Alexis T. Bantle, Joe J. Solvason, Jessica L. Grudzien, Agnieszka D'Antonio-Chronowska, Fabian Lim, Sophia H. Le, Benjamin P. Song, Michelle F. Ragsac, Adam Klie, Reid O. Larsen, Kelly A. Frazer and Emma K. Farley

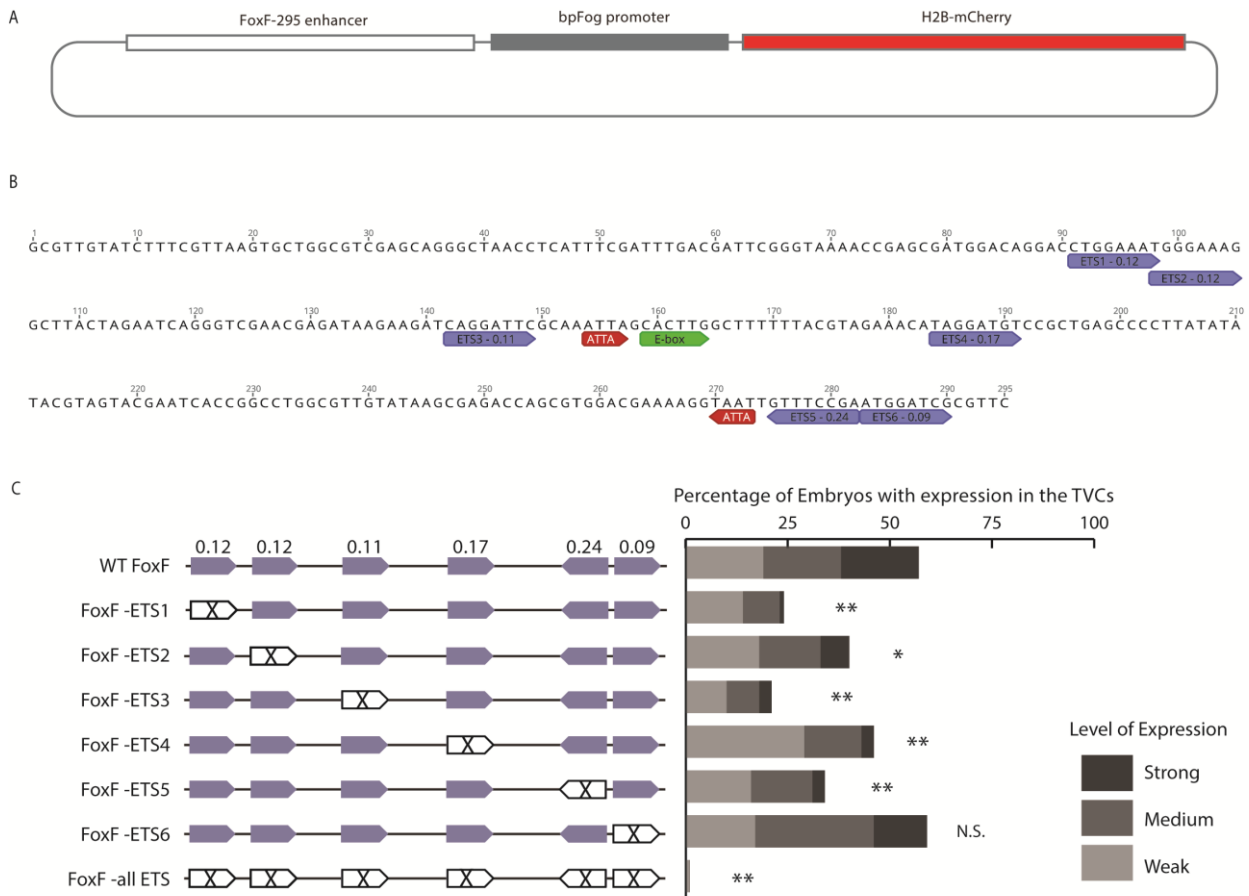


Figure S1. Counting data for ETS site ablation within the FoxF enhancer. Related to Figure 1.
A. Schematic of FoxF enhancer reporter construct. **B.** Sequence of the 295bp FoxF enhancer with transcription factor binding sites found by previous studies and the current study. Previously studied EtsA, EtsB, and EtsC sites are described as the ETS3, ETS4, and ETS5 sites. **C.** Schematics show the enhancers that were electroporated into embryos. Diagrams indicate the WT FoxF fragment and X indicates GGAW > GCAW mutation. Graph shows the proportions of embryos and levels of expression in TVCs (3 replicates, $n \geq 50$ embryos for each replicate). P values are obtained by using Chi-square test comparing each condition to the WT FoxF enhancer with Bonferroni correction: ** $P < 0.0007$, * $P < 0.007$, N.S. not significant. Data in stacked bar chart are represented as the mean. Table S1 contains sequences of ETS sites in each construct. Figure S2 contains representative images for each of these constructs.

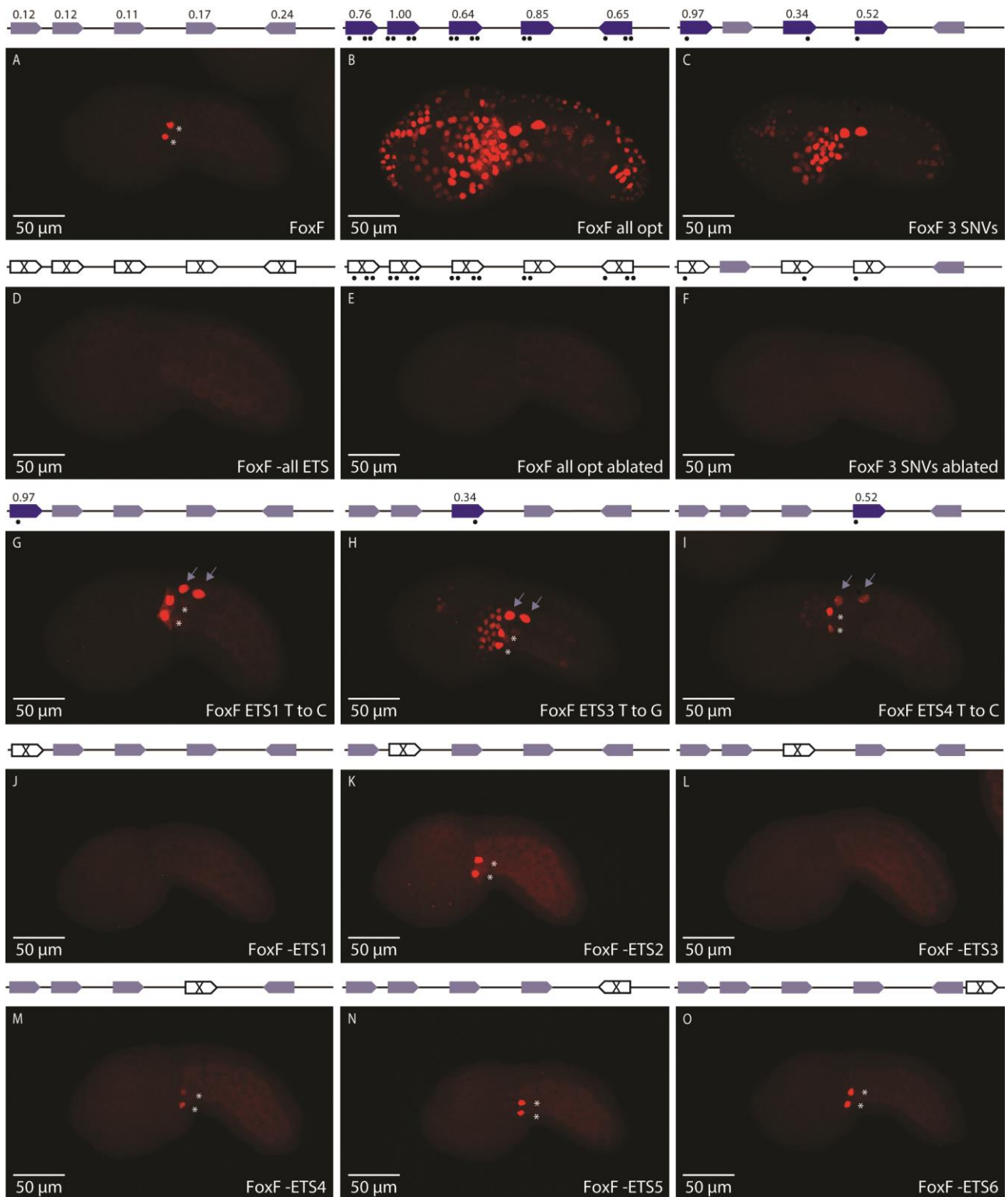


Figure S2. Representative images of each of the FoxF constructs tested in this study. Related to Figures 1 and 2. The first nine images are alternate representative images to those included in the main figures. The final six images are representative images for the single-site ablation constructs in Figure S1. The counting data for FoxF -ETS1 and FoxF -ETS3 shows fluorescence in less than 25% of embryos, therefore we included embryos with no fluorescence as representative images. Scale bars, 50 μ m.

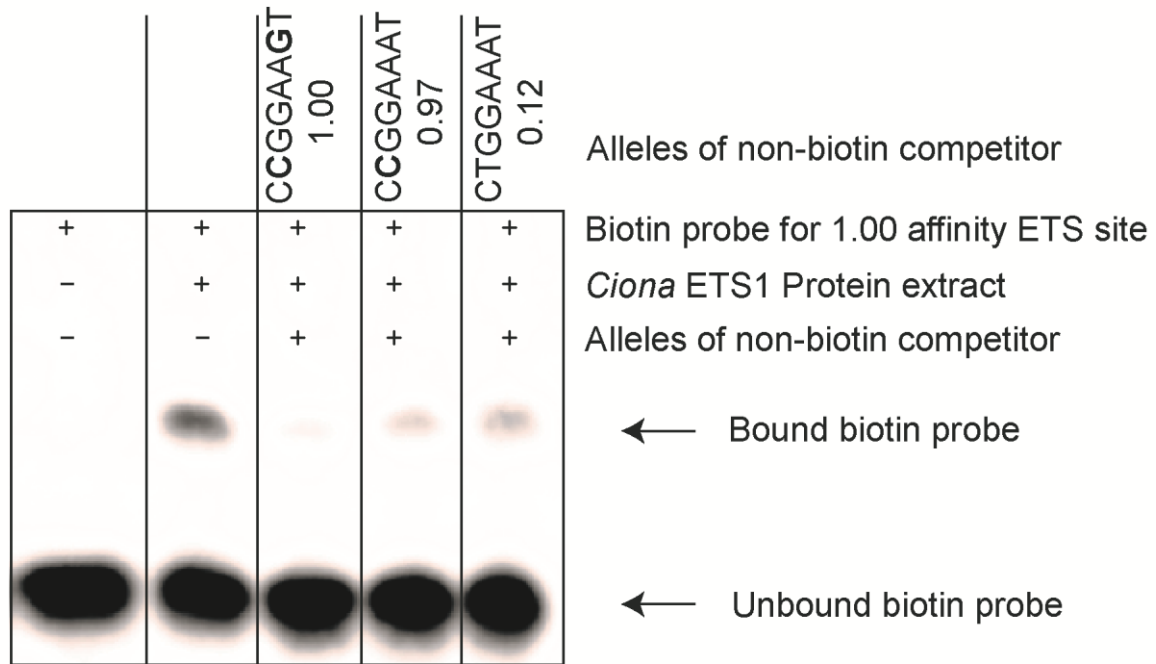


Figure S3. Differential binding affinity with ETS1 single nucleotide variant. Related to Figure 2. We performed an EMSA to detect binding of *Ciona* ETS1 DNA Binding Domain (DBD) to a biotin labelled 30bp sequence of the FoxF enhancer centered on ETS1 with a 1.0 affinity site. We compared the impact of unbound competitor alleles containing the ETS site of 1.0 affinity, the 0.97 ETS1-T-to-C site and the WT ETS1 site. *Ciona* ETS1 DBD bound to the 1.0 ETS binding site in the control probe (lane 2) and this specific binding was competed most effectively by the unlabeled competitor with the 1.0 affinity site (lane 3). The unlabeled competitor probe harboring the single nucleotide variant ETS1-T-to-C competed almost as efficiently as the probe harboring a 1.0 affinity ETS site (lane 4), while probe harboring the wild-type ETS1 site was the least efficient at competing binding to the labelled probe (lane 5).

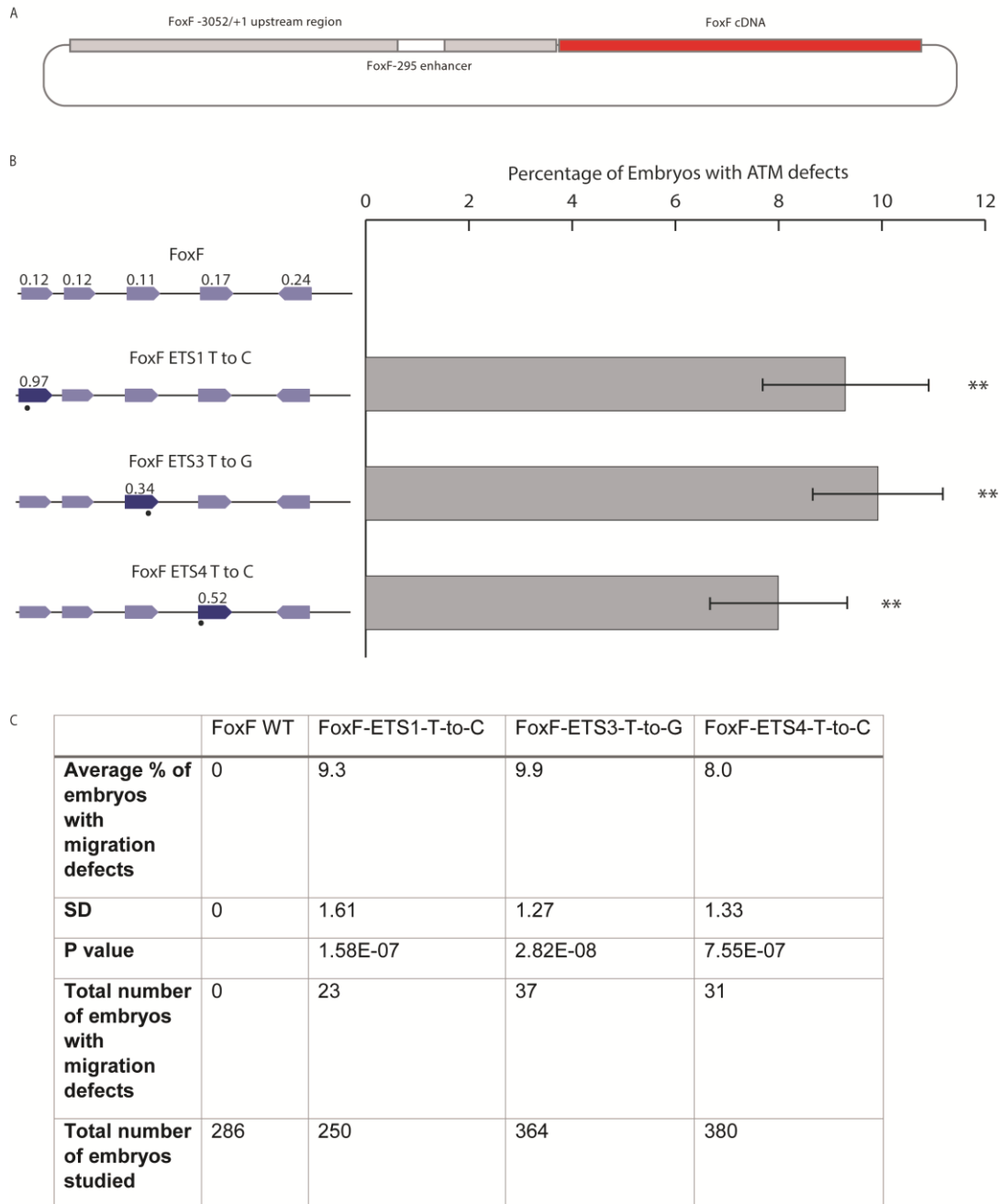


Figure S4. Counting of migration defects in tailbud embryos with affinity-optimizing mutations. Related to Figure 3. A. Schematic of FoxF enhancer *FoxF*cDNA construct. **B.** Bar chart of percentage of embryos with ATM migration defects. We scored the migration of ATMs into the ventral midline in between 250 and 380 embryos per condition. P-values are obtained by using Chi-square test comparing to WT FoxF enhancer with Bonferroni correction: ** P < 0.0017. The single nucleotide variants made are shown by the dots in the enhancer schematic. Data are represented as mean \pm standard deviation. **C.** Table with number of embryos. We analyzed five replicates for WT, three for FoxF-ETS1-T-to-C and two replicates each for FoxF-ETS1-T-to-G and FoxF-ETS4-T-to-C. N values for FoxF WT are 34, 36, 47, 81, and 88. N values for FoxF-ETS1-T-to-C are 96, 60, and 94. N values for FoxF-ETS3-T-to-G are 231 and 133. N values for FoxF-ETS4-T-to-C are 224 and 156.